Protein dynamics viewed by hydrogen exchange

John J. Skinner,[1]*† Woon K. Lim,[2] Sabrina Bédard,[1] Ben E. Black,[1] and S. Walter Englander[1]

[1]Johnson Research Foundation, Department of Biochemistry and Biophysics, Perelman School of Medicine, University of Pennsylvania, Philadelphia, Pennsylvania 19104-6059

[2]Department of Molecular Biology, College of Natural Sciences, Pusan National University, 30 Jangjeon-dong, Keumjeong-gu Busan 609-735, South Korea

Received 13 February 2012; Accepted 9 April 2012
DOI: 10.1002/pro.2081
Published online 27 April 2012 proteinscience.org

Abstract: To examine the relationship between protein structural dynamics and measurable hydrogen exchange (HX) data, the detailed exchange behavior of most of the backbone amide hydrogens of Staphylococcal nuclease was compared with that of their neighbors, with their structural environment, and with other information. Results show that H-bonded hydrogens are protected from exchange, with HX rate effectively zero, even when they are directly adjacent to solvent. The transition to exchange competence requires a dynamic structural excursion that removes H-bond protection and allows exposure to solvent HX catalyst. The detailed data often make clear the nature of the dynamic excursion required. These range from whole molecule unfolding, through smaller cooperative unfolding reactions of secondary structural elements, and down to local fluctuations that involve as little as a single peptide group or side chain or water molecule. The particular motion that dominates the exchange of any hydrogen is the one that allows the fastest HX rate. The motion and the rate it produces are determined by surrounding structure and not by nearness to solvent or the strength of the protecting H-bond itself or its acceptor type (main chain, side chain, structurally bound water). Many of these motions occur over time scales that are appropriate for biochemical function.

Keywords: hydrogen exchange; HX; static and dynamic; protein folding; protein dynamics; Staphylococcal nuclease

Introduction

The naturally occurring exchange of protein and water hydrogens depends on and therefore can provide detailed information about structural dynamics, biophysical properties, and functional behavior of protein molecules. This capability is widely exploited in current protein studies.[1,2] It is often conceived that the static and dynamic determinants of protein hydrogen exchange (HX) rates and behavior are well understood, but this is not true. The lack of detailed understanding diminishes the interpretive power of the many important studies that are now being done.

In searching for the structural factors that determine HX slowing, prior workers have attempted top down strategies. One hypothesizes some broad general determinant and then tests an HX database for correlation with that factor. To explain unexpectedly slow exchange at the protein surface, factors considered have included relative solvent exposure[3,4] and electrostatic field.[5,6] For

Additional Supporting Information may be found in the online version of this article.

Grant sponsor: NIH; Grant numbers: GM031847, GM082989; Grant sponsor: NSF; Grant number: MCB1020649; Grant sponsors: Mathers Foundation, Burroughs Welcome Fund (Career Award in the Biomedical Sciences), Rita Allen Foundation Scholars Award; Grant sponsor: Pusan National University Bio-Scientific Research Grant; Grant number: PNU-2010-101-245.

†Current address: Department of Biochemistry and Molecular Biology, University of Chicago, Chicago, Illinois 60637.

*Correspondence to: John J. Skinner, GCIS Room W107E, 929 E. 57th St., Chicago, IL 60637.
E-mail: skinnerj@uchicago.edu

more buried hydrogens, factors considered have included solvent penetration into the protein, degree of burial, H-bonding, local packing density, and transient unfolding reactions.[3,7–11] In previous work we compared these models with an HX dataset that covers the entire HX range of the amide hydrogens of the well-studied α/β protein, Staphylococcal nuclease (SN).[12] Predictive success was not impressive.

We take a bottom up approach and attempt to discern HX mechanism at an amino acid level by examining the HX behavior of individually resolved residues, their neighbor relationships, and their structural context. SN is sufficiently large and structurally varied that it provides a good sampling of the various possible HX mechanisms. An extensive HX dataset and related information makes it possible to pursue a systematic examination. The results emphasize the role of H-bonding protection and illuminate several modes by which dynamic local and larger protein motions can relieve structural protection. Size scales range from a crankshaft motion about a pair of alpha carbons to the cooperative unfolding of the entire protein, and time scales (frequency of occurrence) range from milliseconds to days.

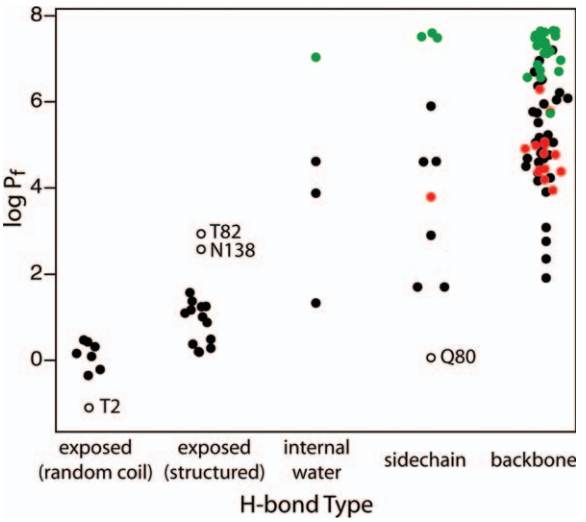

Figure 1. H-bonding inventory showing measured log protection factor versus H-bond acceptor. Symbols indicate amide hydrogens known to exchange by way of a large unfolding reaction (green), or a small local fluctuation (red), or whether this information is not available (black). Amides that H-bond to solvent are separated by whether they reside on well-structured or unstructured regions of main chain. Open circles identify cases explained in the main text. Data can be found in Table S1.

Results

In order to compare residue-resolved HX rates with the details of SN structure (PDB: 1SNO) and with their local and long range relationships, we obtained an HX dataset for most of the amide hydrogens of the SN double mutant, P117G/H124L.[12] The mutant protein has increased stability (10 kcal/mol vs. 6 kcal/mol for WT) so that the exchange of most hydrogens is not dominated by transient global unfolding. We used different NMR methods that can access faster and slower HX rate windows, and varied ambient conditions to bring faster and slower exchanging hydrogens onto the laboratory time scale.

The detailed HX information is supplemented by knowledge of the sensitivity of the exchange of SN hydrogens to external conditions.[13,14] Hydrogens that are exposed to exchange by sizeable unfolding reactions and by much smaller structural excursions, referred to as local fluctuations, can be distinguished by their relative sensitivity to added denaturant.[15–17] Independently, the observation that some amide hydrogens can enter the EX1 HX regime at elevated pH where rate becomes pH independent (see Discussion) distinguishes sizeable unfolding reactions[18] that refold slowly (>1 ms), since local fluctuations can reclose much faster.[19]

H-bonding

Examination shows that nearly all of the amide hydrogens in SN are involved in H-bonding. This seems to be true of proteins in general because the incorporation of a non-H-bonded amide incurs a cost of several kcals in stabilization free energy.[20] Figure 1 presents an inventory of H-bond acceptors, most often main chain or side chain groups of the protein. Some amides form H-bonds to a crystallographically defined water molecule, which can be internal or can interact with bulk solvent. For some surface amides classified as exposed, no H-bonding partner or interacting water is seen in the crystal structure, presumably due to translational freedom or to lattice contacts.

Eight measured SN amides are in unstructured segments near the protein termini that are not defined in the X-ray structure but do produce sharp NMR lines, indicating high mobility. They exchange at close to their expected freely exposed rates[21] with HX protection factor ~1 [log $P_f \sim 0$), where P_f is defined as the degree of slowing relative to the expected freely exposed rate; Eq. (2)]. Interestingly, however, surface-exposed amides on structured segments, although H-bonded to solvent water, exchange more slowly with P_f between 1.5 and 38.

Amides protected by H-bonding to backbone carbonyls, side chains, or structurally incorporated water molecules exchange far more slowly (Fig. 1). Each type spans essentially the entire HX rate range, almost eight orders of magnitude wide, indicating that HX slowing is not determined by the H-bond type.

The secondary structural elements of SN include a distorted five-stranded β-barrel, three major α-helices, and connecting loops. Figures 2–5

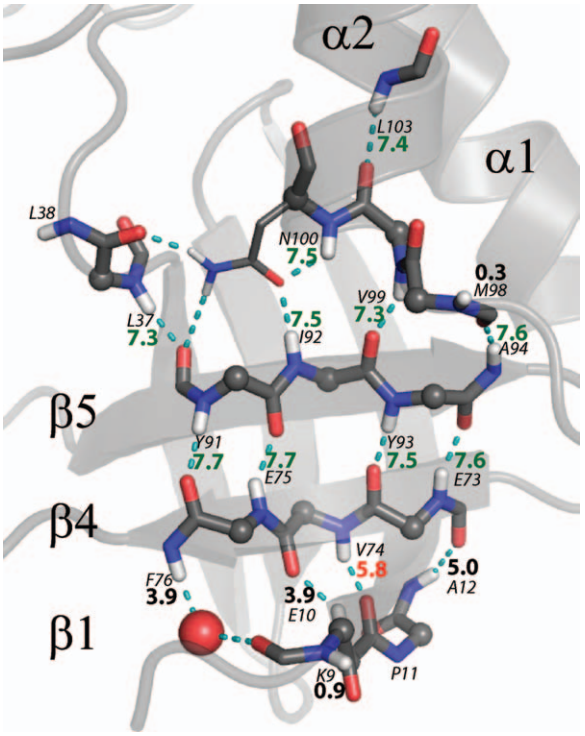

Figure 2. Global unfolding on one face of the β-barrel. Standard colors and stick diagrams identify main chain atoms superimposed on secondary structural elements and connecting loops diagrammed as background. H-bond donors and acceptors are indicated. Log of protection factors are in colors as in Figure 1, indicating HX by way of unfolding (green), local fluctuations (red), or unknown (black). The red sphere is a crystallographically defined water molecule.

show regions of the SN structure, with H-bond donors and acceptors and the log P_f measured for each amide hydrogen. In many of these cases, examination of the pattern of exchange of neighboring residues indicates the dynamic structural distortion that allows exchange.

Global unfolding in the β-barrel

Figure 2 shows amides H-bonded on one face of the five-stranded SN β-barrel. The surface of the β-structure is in direct contact with water. For example, the Met98 and Lys9 amides face into solvent and exchange at near the free peptide rate ($P_f = 2$ and 10). Other closely neighboring amides, also at the aqueous surface, exchange more slowly by 10 million-fold. Thus, direct contact with solvent does not ensure rapid exchange. These observations are at odds with the widely held concept that HX rates relate to static solvent exposure, and they limit the time scale of any possible mechanism for direct transfer from the static structure to immediately proximal solvent to many days.[13]

These hydrogens exchange slowly because they are protected by H-bonding. They are variably H-bonded between β strands, within a helix, and even with a side chain (Asn100), and their H-bond acceptors are diverse, including main chain carbonyls, a side chain, and a crystallographically defined water molecule. Nevertheless, they all exchange within a narrow range, with log $P_f = 7.3$ to 7.7. Evidently, they are exposed to solvent by the same large distortion that exposes all of these hydrogens together. In agreement, their exchange exhibits a sharp dependence on denaturant,[14] suggesting a large scale unfolding. The measured P_f values correspond to an unfolding free energy of 10 kcal/mol, equal to the global protein stability [Eq. (3)]. At pH 8.5 and above,[13] the very slow hydrogens deviate towards pH independence (EX1 HX) consistent with

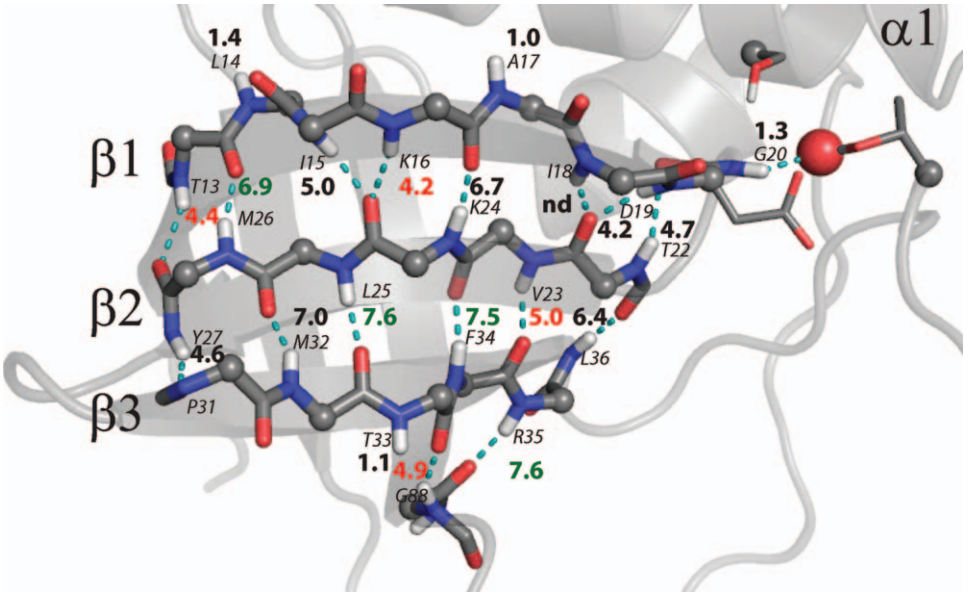

Figure 3. Heterogeneous exchange on the other face of the β-barrel. The identification scheme is as described for Figure 2.

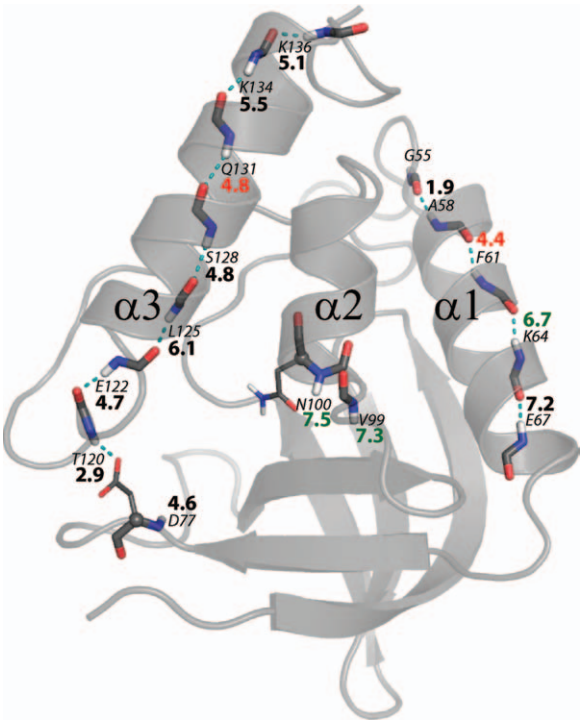

Figure 4. Varied exchange mechanisms in the three α-helices. The identification scheme is as described for Figure 2.

a large unfolding - slow refolding HX mechanism, in this case with a reclosing rate $\sim 10^2$ s^{-1}, close to the rate for the first folding phase in refolding from the denatured state.[22] These results consistently indicate that the HX exposure reaction is the reversible global unfolding/refolding reaction under native conditions.

These results have broad general significance. They validate an implicit two-state assumption of the Linderstrøm-Lang model (Scheme 1), namely hydrogens alternate between states that are exchange competent and protected states where the effective HX rate is zero. For sites just discussed, measured HX is slowed by almost eight orders of magnitude even though the hydrogens are at the aqueous protein surface. Their exchange requires a structural distortion that separates protecting H-bonds and exposes the hydrogens to attack by solvent HX catalyst. These same conclusions appear to be true for protected hydrogens in general.

Local dynamic exposure in the same β-barrel structure

Amides H-bonded between β4 and β1 are protected by very similar structure but they exchange with varied faster rates (log P_f = 3.9–5.8), suggesting diverse smaller H-bond breaking structural fluctuations. Fluctuations that expose the amide NHs of Val74 and Phe76 (on β4) clearly involve their H-bond acceptors (β1 and water) and not these residues themselves. This follows from the fact that peptide groups are rigidly planar. Displacement of the β4 amide NHs themselves would equally displace their carbonyls and separate the H-bonds that protect several β5 residues, but the β5 residues are seen to exchange much more slowly. Therefore, β4 must remain in place through these fluctuations. The exchange of Val74 and Phe76 appears to involve a small fraying motion that displaces their acceptors

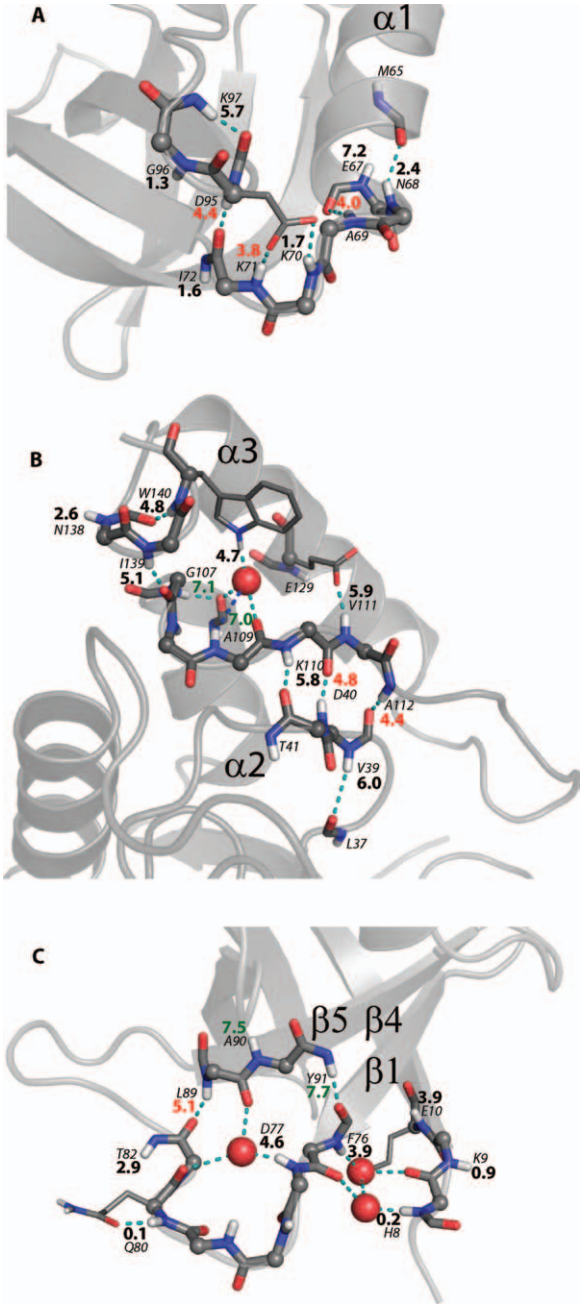

Figure 5. Loop regions and defined water molecules. The identification scheme is as described for Figure 2. (A) The α1/β4 loop, (B) the α2/α3 loop, α1/β3 loop, and C-terminal region, and (C) the β4/β5 loop and near C-terminal region. Asn138 (B) was reoriented in NMR (2KQ3). Thr82 was involved in a crystal lattice contact (1SNO).

near the N-terminus of β1. In agreement, Val74 has zero dependence on denaturant, consistent with exchange by a local fluctuation.

Similar local motions are presumably possible for the much slower hydrogens, but the data require that such local modes could only provide an even slower exchange pathway than is accomplished by global unfolding. What inhibits local fluctuations? Note the very slow exchange of hydrogens protected by the side chain of Asn100. The Asn100 side chain provides strong protection because it is rigidly held in place, packed between a sheet and a helix that are well packed. Evidently, similar rigidity and resistance to local fluctuations extends to the β4 and β5 strands.

Heterogeneous exchange in the β-barrel

Figure 3 shows the opposite face of the β-barrel, starting farther along β1 as it wraps around the barrel. As before, H-bonded hydrogens are well protected even though most of this surface is in direct contact with solvent, but here the HX pattern is varied. Some hydrogens exchange very slowly with denaturant dependence and EX1 behavior indicative of a concerted unfolding reaction (shown in green). Other immediately neighboring residues undoubtedly experience the same large unfolding but they exchange more rapidly, indicating exchange by more probable small fluctuations in which the major strands remain in place. In agreement, the denaturant dependence measured for some of these faster residues is negligible (red).

Val23 (on β2) is particularly interesting in that the detailed motion that permit sits exchange can be inferred by the local context. Given the rigid planarity of the peptide bond and the significantly higher P_f values of most of its neighboring residues, the motion that exposes Val23 to exchange cannot involve those residues (Lys24 on β2; Phe34, Leu36, and Arg35 acceptors on β3). These observations seem to require that the Val23 amide is exposed to solvent by a crankshaft rotation of the Thr22/Val23 peptide group about its two neighboring α-carbons. This state unfavorably inserts the Thr22 carbonyl into the hydrophobic center of the β-barrel which contributes to the fact that it is only populated 10^{-5} of the time.

Why are local fluctuations similar to Val23 not seen throughout the β-barrel? The only remarkable characteristic of the Thr22/Val23 peptide group is that the carbonyl accepts two H-bonds. An identical situation is seen for the Lys24/Leu25 peptide group, but Leu25 exchanges much more slowly and requires a large unfolding reaction. Apparently the difference is side chain-dependent. Between Lys24 and solvent there is a pocket of large hydrophobic side chains with the charged end of the Lys24 side chain acting as a polar cap. In contrast, side chains do not obstruct water accessibility to Val23. These observations again stress that exchange of protected hydrogens requires both H-bond separation and solvent exposure.

Several amides at the sheet edge—Leu14 and Ala17 on β1 and Thr33 on β3—are fully exposed to external water. As noted before (Fig. 1), P_f values for these unprotected hydrogens on structured segments are modestly larger than for hydrogens on unstructured segments (P_f = 10, 20, and 25). Gly20 on β1 is bound to a water that is held by two side chains which however seem freely mobile and provide very little protection.

Helices

Figure 4 shows the three SN α-helices. Each exhibits a different HX pattern, evidently modulated by surrounding structure. In α1, log P_f values for the H-bonded amides from residue 58 to 69 are as follows: 1.9, 3.1, nd, 4.4L, 5.7U, 6.7, 6.7U, 6.6U, 7.0U, 7.2, 2.4, 4.0L, 1.7. L and U indicate known dependence on local fluctuations and unfolding, respectively. H-bonded amides through the middle of the helix, on both the aqueous and inner surfaces, have similar P_f and a large denaturant dependence, indicating a cooperative whole helix unfolding reaction. The more N-terminal helical residues presumably participate in the same cooperative whole helix unfolding but their exchange is dominated by more facile opening reactions which produce a fraying progression, with low denaturant dependence apparently due to small surface exposure in the fray. No fraying pattern is seen for the α1 C-terminus which is stabilized by a capping interaction [see Fig. 5(A)].

In helix α2, residues 102–109 exchange by way of a large unfolding reaction, with high denaturant dependence but with smaller stability (ΔG_{op} from EX2 HX) and faster unfolding rate (from EX1 HX) than for the global unfolding. Unlike the other helices, no faster exchange due to local fluctuations is seen, perhaps because α2 is packed between the other helices. One expects that the α2 N-terminal residues 99 and 100 will participate in the same cooperative subglobal unfolding as the rest of α2 but they are even slower, remaining protected until global unfolding exposes them along with β5 (see Fig. 2).

In contrast, the α3 amides show disparate rates and so do not exchange by a cooperative helix unfolding. Log P_f for residues Glu122 to Leu137 are: 4.7, 0.2, 1.3, 6.1, 6.3L, 4.2, 4.8L, nd, 6.1, 4.8, 6.5, 6.2, 5.5, 5.0L, 5.0, 5.2. An oscillating HX rate pattern rises and falls with a rough helical periodicity as the residues go from buried (with α2) to solvent exposed and back again. The variability in P_f values indicates that local fluctuations predominate. The repeated return to a common high log P_f value (6.1–6.5) is suggestive of a cooperative helix unfolding.

However, Arg 126 (log P_f = 6.3L) lacks denaturant dependence, indicating a local fluctuation. Given the observation of cooperative unfolding of helices α1 and α2, one might expect α3 to behave similarly. If so, this mode is hidden by the fact that local fluctuations provide faster HX pathways than for any cooperative α3 unfolding which must occur less than $10^{-6.3}$ of the time.

Loops and water

Figure 5(A) depicts HX behavior in the short α1/β4 loop. Three neighboring amides, two within the loop (Ala69 and Lys71) and one on an adjoining loop (Asp95), with varied H-bonding (backbone, side chain), have similar protection factors (log P_f = 4.0, 3.8, 4.4) suggesting that they may be exposed together by a concerted loop unfolding. All three residues exhibit low denaturant dependence because the loop is so small (as for β3 fraying in Fig. 3). The concerted unfolding of loops has been noted before[23] and may reflect a common dynamic mode.

The intervening loop residue, Lys70, exchanges much faster (log P_f = 1.7), indicating a local motion in which the 69/70 peptide group is separately exposed, apparently by a crankshaft rotation about the two neighboring alpha carbons. Other alternatives are ruled out by the slow exchange of Lys71 and Lys97 amides and their protecting groups.

Figure 5(B) shows residue interactions in the α2/α3 loop, the α1/β3 loop, and the near C-terminal region (residues 141–149 are unstructured). A defined water molecule mediates the interaction between α3 and the α2/α3 loop. It is held in place by four H-bonds, donating to two main chain carbonyls and accepting two others (from the indole ring NH of Trp140 and the amide NH of Ala109; C-termini of α3 and α2, respectively). This and other internal SN waters are found in irregular loop structures where they satisfy H-bonding requirements. In these cases the local context indicates that none of the donor hydrogens exchange by way of the water simply diffusing away. The Ala109 amide to water H-bond is unusually long, 4.4 Å N to O, but no other available acceptor is present. In spite of its long H-bond, Ala109 is highly protected (log P_f = 7.0), indicating that H-bond strength is not a determinant. The hydrogen ultimately exchanges as part of the cooperative α2 helix unfolding. The Trp140 indole ring NH is less protected and may exchange through the same local motion that exposes its similarly protected backbone (log P_f = 4.7 and 4.8).

In the α1/β3 loop, residues Asp40 and Ala112 are similarly protected (log P_f = 4.8 and 4.4) and are surrounded by another set of residues (Val39, Lys110, Val111) with similar protection (log P_f = 6.0, 5.8, 5.9). Nevertheless, the HX pattern points to separate residue motions with the similarities probably arising by chance from unrelated, independent motions.

Figure 5(C) shows the long β4/β5 loop and its interaction with the near N-terminal region. A number of interactions are mediated by water molecules. His8, proximal to the unstructured N-terminal segment, H-bonds to a defined water. The water is in direct contact with bulk, and protection is low (P_f < 2). In contrast the immediately neighboring water strongly protects Phe76 (log P_f = 3.9) even though it is only one water removed from bulk. The water acceptor for Asp77 also offers strong protection (log P_f = 4.6). A crucial determinant seems to be the number of water to protein contacts. Both of the latter waters donate two H-bonds to protein carbonyls, thus their replacement by a hydroxide catalyst, either in place by H-transfer or when the water leaves, would not fulfill the local H-bonding requirements without some structural reorganization.

Structural detail from HX

HX rates may help to resolve some structural ambiguities. Asn138 appears to be H-bonded to external solvent in the crystal structure. However, the measured log P_f of 2.6 is large (Fig. 1), more consistent with the conflicting NMR structure (2KQ3) where Asn138 is reoriented and H-bonds to the Arg105 CO. Again, in the SN X-ray structure, the Gln80 amide appears to be protected by its own side chain but solution HX finds it to be the least protected of all side chain-protected amides (Fig. 1). The X-ray structure finds no H-bond acceptor for the neighboring Thr82, but solution HX data shows that it is the most protected ($P_f \sim 1000$) among exposed amides. Examination of the X-ray data reveals that both anomalies could be reconciled by the suggestion that the Gln80 side chain actually protects Thr82 in solution and not Gln80. The X-ray anomaly occurs because Thr82 interacts with the side chain of a neighboring protein in the crystal lattice. The NMR structure provides no helpful NOE information in this case.

Discussion

In formative work before the first protein structure had been solved and before the dynamic nature of protein molecules had been considered, Linderstrøm-Lang proposed a general model for structurally hindered HX, commonly represented as in reaction Scheme 1.[24–26] The model supposes that hydrogens while protected cannot exchange at all. They must be made exchange competent by unspecified structural transients, defined only kinetically by their structural opening and reclosing rates, k_{op} and k_{cl}.

$$\text{Closed} \underset{k_{cl}}{\overset{k_{op}}{\rightleftarrows}} \text{open} \xrightarrow{k_{ch}} \text{exchange}$$

Scheme 1. Linderstrøm-Lang kinetic model for exchange of protected hydrogens.

In the exposed condition they exchange at some chemical rate, k_{ch}.

This simple kinetic scheme specifies that when structure is stable ($k_{cl} > k_{op}$) and reclosing is relatively fast ($k_{cl} > k_{ch}$), opening and reclosing occur many times before each successful exchange event. HX rate then depends on the fraction of time the open form exists and therefore the structural opening equilibrium constant (K_{op}), as in Eq. (1). In this case, the protection factor can be obtained as in Eq. (2) and the free energy of the responsible unfolding reaction as in Eq. (3). With increasing pH and/or decreasing stability, k_{ch} may exceed k_{cl}. Exchange then approaches a maximum plateau rate equal to k_{op}. These two limiting cases are referred to as EX2 (bimolecular) and EX1 (unimolecular) exchange.[26]

$$k_{ex} = K_{op}/(1 + K_{op})\, k_{ch} \quad (1)$$

$$P_f = (K_{op} + 1)/K_{op} = k_{ch}/k_{ex} \sim 1/(\text{fraction open}) \quad (2)$$

$$\Delta G_{op} = -\text{RT} \ln K_{op} \sim -\text{RT} \ln k_{ex}/k_{ch} \quad (3)$$

Fifty years on, the study of naturally occurring protein HX has matured into a powerful method for learning about the biophysical and functional properties of protein molecules. In this development, Scheme 1 has often served as an aid to interpretation but the static and dynamic factors that determine protein HX remain unclear. The present study contributes some mechanistic information to this kinetic framework. We find information on the exchange of structurally unprotected hydrogens, the role of H-bonding in imposing slowed exchange, and the different classes of dynamic motions that relieve protection, namely segmental unfolding reactions and more local fluctuations. These observations are of interest for the interpretation of HX results in terms of the biophysical properties of protein molecules and their role in protein function.

Unprotected hydrogens

Following an extended development recently reviewed by Baldwin,[27] the details of the amide chemical exchange reaction in the absence of structural protection, encoded as k_{ch} in Scheme 1, are now well understood. Amide HX is catalyzed by hydroxide and hydronium ions[28–30] in proton transfer reactions that involve a direct attack on the amide, formation of a connecting H-bond, equilibration of the hydrogen between donor and acceptor, and final separation of the encounter complex.[31] Exchange from a freely exposed amide in random coil structure depends on parameters that have been accurately calibrated (pH, temperature, neighboring side chains, isotope effects) so that HX rates for any given condition are predictable.[21,32] For residues in unstructured protein regions, agreement with predicted values is found, here and by others.[33,34–36] This knowledge makes it possible to compute K_{op}, P_f, and ΔG_{op} from measured k_{ex} [Eq. (1–3)].

In these calculations, it has always been assumed that k_{ch} in Scheme 1 is equal to the predicted random coil value. The present work finds a new factor. When the exposed amide is placed on a rigidly structured segment, its exchange tends to be slower than the random coil expectation by roughly 10-fold (factors of 2- to 40-fold measured; Fig. 1). This will exaggerate the value of ΔG_{op} when it is calculated as in Eq. (3). In addition, it may help to explain the range of P_f that is often seen among multiple residues exposed to exchange by a given unfolding reaction.

The role of H-bonding

It is often supposed that surface exposed hydrogens will exchange rapidly. This view is incorrect. For example, the diverse residues and interactions in Figure 2 are vicinal to solvent. Non-H-bonded hydrogens exchange at close to the expected free peptide rate, but immediately neighboring hydrogens that are protected by H-bonding are highly protected and exchange more slowly by many orders of magnitude.

We find that the degree of HX protection does not simply depend on surface exposure, depth of burial, H-bond strength (length), or H-bond acceptor type which can be a main chain carbonyl, a side chain, or even a bound water.[12] For each type of acceptor, the degree of protection covers the entire range of energetics (Fig. 1). The determining parameters appear to be the difficulty of separating the H-bond in a way that makes the hydrogen accessible to attack by solvent HX catalyst and the stability of the distributed interactions that inhibit that perturbation. Any given hydrogen might exchange by many alternative pathways ranging from small amino acid level distortions to whole molecule unfolding. The exchange rate observed is determined by the H-bond breaking motion that provides the fastest exchange.

Protection by water

The present results reveal that even H-bonding to water molecules that are held in place by protein interactions can block exchange. Replacement of bound water by hydroxide can be very unfavorable depending on the interactions involved and the structural reorganization required.[37] HX protection by bound water can be compared with analogous protection by protein groups and will not depend on the frequency of water dissociation, as in Scheme 1 under EX2 conditions.

In previous work, some surface-exposed hydrogens in several proteins were found to be slowed by up to one billion-fold, and this was attributed to local electrostatic effects.[6] However, the protection due to defined water molecules seen here raises the possibility that the slowing observed before might be due to steric protection by structurally held water

molecules. When solvent is treated as a continuum as in the earlier studies,[5,6] near-surface structurally bound waters will not be distinguished from free solvent. An analysis of the earlier examples shows that the very slow surface hydrogens are often H-bonded to crystallographically defined water molecules held in place by protein interactions.[12]

Unfolding reactions

In earlier HX work, it was proposed[38,39] and later demonstrated[40,41] that proteins unfold and refold repeatedly even under native conditions, and that the transient global unfolding reaction governs exchange of the slowest hydrogens in many proteins.[42,43] Subsequently, the reversible unfolding of cooperative subglobal structural units called foldons was found.[16,36,44–52] These most interesting dynamic entities can be identified and characterized when they determine measurable HX behavior.

In the present work, cooperative unfolding reactions were recognized by the observation that contiguous sets of hydrogens exchange with the same protection factor (EX2 regime) and even with the same unfolding and refolding rates (EX1 regime). A major SN unfolding reaction was detected by the concerted exchange of residues on one side of the β-barrel and some near neighbors. These sites are so well protected that they exchange only by way of global unfolding. Two of the three helices in SN and a small loop were seen to experience concerted subglobal unfolding reactions. Cooperative subglobal foldon units have been seen in other proteins, involving helices, parts of β-structure, loops, and groupings thereof. These results indicate that the cooperative unfolding of secondary structural elements represent common dynamic modes of native proteins.

It can be noted that HX measurements of concerted unfolding reactions may identify only some fraction of the residues that actually participate in the unfolding. Direct HX definition of the complete folding/unfolding unit is limited by the fact that additional sites, both peripheral and intervening, and even entire additional segments, may have exchanged earlier by faster pathways. For example, all residues participate in the global unfolding but only those that have resisted exchange through all faster pathways are actually measured to exchange by global unfolding.

Local fluctuations

HX by way of unfolding reactions has often been recognized by its sensitivity to increasing concentrations of denaturant which is well known to promote cooperative unfolding reactions.[17] Sensitivity to other intensive parameters including temperature[53] and pressure[50] has also been demonstrated.

Residues with HX rates that are insensitive to low concentrations of denaturant, implying little change in exposed surface area during the exchange reaction, have been said to exchange by way of local fluctuations. However, the reality of local fluctuations in HX rate determination as opposed to sizeable unfolding reactions has been questioned[11,54,55] based on two possible scenarios. One is that HX rate differences between neighboring residues, which appear to reflect local fluctuations, may in fact represent an overlap of different unfolding reactions. A second is that the intrinsic denaturant sensitivity of given residues may be masked by concomitant denaturant effects elsewhere in the protein.

The present examination of HX in SN provides the most detailed analysis of local fluctuations to date. Some individual residues in SN can be seen to exchange much more rapidly than their sequence neighbors. These observations limit local fluctuations to only one or a few residues in size and cannot be explained by any combination of sizeable unfoldings. Secondly, when sufficiently complete HX patterns of many contiguous residues are available, we find a 1:1 correspondence between multiresidue unfolding behavior and large denaturant sensitivity and between local fluctuational exchange behavior and zero denaturant sensitivity. These results support the reality of local fluctuations and the validity of denaturant sensitivity to distinguish exchange by way of unfolding and local fluctuations. A caveat is that very small unfolding reactions may have little dependence on denaturant.

HX dynamics and protein function

Protein HX occurs on a relatively long time scale. A common misunderstanding is that the determining protein dynamics occurs on a similarly slow time scale. In fact, an unfolding reaction that occurs for example once per second can generate HX times of days [Eq. (1)]. Given Eqs. (1) and (2) and known reclosing rates, one can calculate opening rates (frequency of occurrence) of these structural reactions. For local fluctuations, reclosing time has been estimated in one case at <1 μsec[19]; for unfolding reactions, reclosing times are between $\sim$1 μsec and 10 msec.[18,47,56–58] Therefore, measured K_{op} values span a wide range that includes the ms to s time scale. The time scale and physical size of these motions makes them potentially important for the control of protein interactions and structural transitions.[59–62]

This entire class of protein dynamics is easily accessible to measurement by HX. A limited subset can be also accessed by NMR relaxation dispersion measurements ($K_{op} \geq 0.01$, $k_{op} \sim$ ms),[47] and by long time molecular dynamics calculations ($k_{op} \sim$ ms).[63] This paper illustrates how the comparison of HX data with structural context can be used to characterize large and small protein motions and quantify their equilibrium and kinetic properties. The same

straightforward approach should be applicable to proteins quite broadly.

Materials and Methods

Protein preparation

Experiments used a double mutant version of SN (P117G/H124L) with increased stability, at 10 kcal/mol for the double mutant compared with 6 kcal/mol for WT, so that the exchange of most hydrogens is not dominated by the transient global unfolding. The SN double mutant was expressed and purified as described before.[13]

HX measurement and analysis

NMR HX measurements were collected at 20 °C using a 500 MHz magnet with Varian cold probe. $^{2}H^{15}N$ to $^{1}H^{15}N$ exchange was measured by 2D HSQC in real time over the pH range 7.0–9.5 and by quenched stop flow at pH 9.94 as previously described.[13] Rates were determined by fitting time-dependent cross-peak intensity to a single exponential. ^{1}H-^{1}H exchange was measured using the Cleanex-PM pulse sequence[33] with mixing times of 4, 5, 6, 7, 8, 10, 15, and 20 ms over the pH range 4.9–11.26 at approximately half pH increments. A modified data analysis that provides increased accuracy is described in a previous paper.[12]

Acknowledgments

The authors thank Bertrand García-Moreno, George Rose, Vince Hilser, and Michele Vendruscolo for helpful discussion.

References

1. Konermann L, Pan J, Liu YH (2011) Hydrogen exchange mass spectrometry for studying protein structure and dynamics. Chem Soc Rev 40:1224–1234.
2. Engen J, Jorgensen TJD (2011) Hydrogen exchange mass spectrometry special issue. Int J Mass Spectrom 302:1–2.
3. Woodward C, Li RH (1998) The slow-exchange core and protein folding. TIBS 23:379–379.
4. Truhlar SME, Croy CH, Torpey JW, Koeppe JR, Komives EA (2006) Solvent accessibility of protein surfaces by amide H/H2 exchange MALDI-TOF mass spectrometry. J Am Soc Mass Spectrom 17:1490–1497.
5. LeMaster DM, Anderson JS, Hernandez G (2009) Peptide conformer acidity analysis of protein flexibility monitored by hydrogen exchange. Biochemistry 48: 9256–9265.
6. Anderson JS, Hernandez G, Lemaster DM (2008) A billion-fold range in acidity for the solvent-exposed amides of *Pyrococcus furiosus* rubredoxin. Biochemistry 47:6178–6188.
7. Richards FM (1979) Packing defects, cavities, volume fluctuations, and access to the interior of proteins, including some general comments on surface area and protein structure. Carlsberg Res Commun 44:47–63.
8. Lumry R, Rosenberg A (1975) The mobile defect hypothesis of protein function. Col Int C N R S L'Eau Syst Biol 246:55–63.
9. Tartaglia GG, Cavalli A, Vendruscolo M (2007) Prediction of local structural stabilities of proteins from their amino acid sequences. Structure 15:139–143.
10. Vendrusculo M, Paci E, Dobson CM, Karplus M (2003) Rare fluctuations of native proteins sampled by equilibrium hydrogen exchange. J Am Chem Soc 125: 15686–15687.
11. Wooll JO, Wrabl JO, Hilser VJ (2000) Ensemble modulation as an origin of denaturant-independent hydrogen exchange in proteins. J Mol Biol 301:247–256.
12. Skinner JJ, Lim WK, Bedard S, Black BE, Englander SW (2012) Protein hydrogen exchange: Testing current models. Protein Sci 21:987–995.
13. Bédard S, Mayne LC, Peterson RW, Wand AJ, Englander SW (2008) The foldon substructure of staphylococcal nuclease. J Mol Biol 376:1142–1154.
14. Wrabl JO. Investigations of denatured state structure and *m*-value effects in Staphylococcal nuclease. (1999). USA: The Johns Hopkins University, pp. 199.
15. Bai YW, Englander JJ, Mayne L, Milne JS, Englander SW (1995) Thermodynamic parameters from hydrogen exchange measurements. Energ Biolog Macromol 259: 344–356.
16. Bai Y, Sosnick TR, Mayne L, Englander SW (1995) Protein folding intermediates: native-state hydrogen exchange. Science 269:192–197.
17. Pace CN (1986) Determination and analysis of urea and guanidine hydrochloride denaturation curves. Methods Enzymol 131:266–280.
18. Hoang L, Bédard S, Krishna MMG, Lin Y, Englander SW (2002) Cytochrome *c* folding pathway: kinetic native-state hydrogen exchange. Proc Natl Acad Sci USA 99:12173–12178.
19. Hernandez G, Jenney FE, Adams MWW, LeMaster DM (2000) Millisecond time scale conformational flexibility in a hyperthermophile protein at ambient temperature. Proc Natl Acad Sci USA 97:3166–3170.
20. Fleming PJ, Rose GD (2005) Do all backbone polar groups in proteins form hydrogen bonds? Protein Sci 14:1911–1917.
21. Bai Y, Milne JS, Mayne L, Englander SW (1993) Primary structure effects on peptide group hydrogen exchange. Proteins 17:75–86.
22. Maki K, Ikura T, Hayano T, Takahashi N, Kuwajima K (1999) Effects of proline mutations on the folding of Staphylococcal nuclease. Biochemistry 38:2213–2223.
23. Krishna MMG, Lin Y, Rumbley JN, Englander SW (2003) Cooperative omega loops in cytochrome c: role in folding and function. J Mol Biol 331:29–36.
24. Linderstrøm-Lang KU, Schellman JA. Protein structure and enzyme activity. In: Boyer PD, Lardy H, Myrback K, Eds. (1959) The enzymes. New York: Academic Press, pp 443–510.
25. Linderstrøm-Lang K. Deuterium exchange and protein structure. In: Neuberger A, Ed. (1958) Symposium on protein structure. London: Methuen.
26. Hvidt A, Nielsen SO (1966) Hydrogen exchange in proteins. Adv Protein Chem 21:287–386.
27. Baldwin RL (2011) Early days of protein hydrogen exchange: 1954–1972. Proteins 79:2021–2026.
28. Berger A, Linderstrøm-Lang K (1957) Deuterium exchange of poly-D,L-alanine in aqueous solution. Arch Biochem Biophys 69:106–118.
29. Molday RS, Kallen RG (1972) Substituent effects on amide hydrogen exchange rates in aqueous solution. J Am Chem Soc 94:6739–6745.
30. Perrin CL (1989) Proton exchange in amides: surprises from simple systems. Acc Chem Res 22:268–275.

31. Eigen M (1964) Proton transfer, acid-base catalysis, and enzymatic hydrolysis. Angew Chem Intl Ed Engl 3:1–19.
32. Connelly GP, Bai Y, Jeng MF, Englander SW (1993) Isotope effects in peptide group hydrogen exchange. Proteins 17:87–92.
33. Hwang TL, van Zijl PC, Mori S (1998) Accurate quantitation of water-amide proton exchange rates using the phase-modulated clean chemical exchange (cleanex-pm) approach with a fast-HSQC (fHSQC) detection scheme. J Biomol NMR 11:221–226.
34. Roder H, Wagner G, Wuthrich K (1985) Individual amide proton exchange rates in thermally unfolded basic pancreatic trypsin inhibitor. Biochemistry 24:7407–7411.
35. Buck M, Radford SE, Dobson CM (1994) Amide hydrogen exchange in a highly denatured state. Hen egg-white lysozyme in urea. J Mol Biol 237:247–254.
36. Koide S, Jahnke W, Wright PE (1995) Measurement of intrinsic exchange rates of amide protons in a N15-labeled peptide. J Biomol NMR 6:306–312.
37. Marx D, Chandra A, Tuckerman ME (2010) Aqueous basic solutions: hydroxide solvation, structural diffusion, and comparison to the hydrated proton. Chem Revs 110:2174–2216.
38. Rosenberg A, Chakravarti K (1968) Studies of hydrogen exchange in proteins. I. The exchange kinetics of bovine carbonic anhydrase. J Biol Chem 243: 5193–5201.
39. Woodward CK, Hilton BD, Tuchsen E (1982) Hydrogen exchange and the dynamic structure of proteins. Mol Cell Biochem 48:135–160.
40. Loh SN, Prehoda KE, Wang J, Markley JL (1994) Measuring global and local structural free energy changes in Staphylococcal nuclease by NMR-observed hydrogen exchange. Tech Protein Chem V:431–438.
41. Bai Y, Milne JS, Mayne L, Englander SW (1994) Protein stability parameters measured by hydrogen exchange. Proteins 20:4–14.
42. Huyghues-Despointes BM, Scholtz JM, Pace CN (1999) Protein conformational stabilities can be determined from hydrogen exchange rates. Nature Struct Biol 6: 910–912.
43. Huyghues-Despointes BM, Pace CN, Englander SW, Scholtz JM (2001) Measuring the conformational stability of a protein by hydrogen exchange. Methods Mol Biol 168:69–92.
44. Chamberlain AK, Marqusee S (2000) Comparison of equilibrium and kinetic approaches for determining protein folding mechanisms. Adv Protein Chem 53: 283–328.
45. Silverman JA, Harbury PB (2002) The equilibrium unfolding pathway of a (beta/alpha)(8) barrel. J Mol Biol 324:1031–1040.
46. Bollen YJM, Sanchez IE, van Mierlo CPM (2004) Formation of on- and off-pathway intermediates in the folding kinetics of azotobacter vinelandii apoflavodoxin. Biochemistry 43:10475–10489.
47. Korzhnev DM, Kay LE (2008) Probing invisible low-populated states of protein molecules by relaxation dispersion NMR spectroscopy: an application to protein folding. Acc Chem Res 41:442–451.
48. Zhou Z, Feng H, Bai Y (2006) Detection of a hidden folding intermediate in the focal adhesion target domain: implications for its function and folding. Proteins 65:259–265.
49. Feng HQ, Vu ND, Bai YW (2005) Detection of a hidden folding intermediate of the third domain of PDZ. J Mol Biol 346:345–353.
50. Fuentes EJ, Wand AJ (1998) Local stability and dynamics of apocytochrome b562 examined by the dependence of hydrogen exchange on hydrostatic pressure. Biochemistry 37:9877–9883.
51. Fuentes EJ, Wand AJ (1998) Local dynamics and stability of apocytochrome b562 examined by hydrogen exchange. Biochemistry 37:3687–3698.
52. Weinkam P, Zong C, Wolynes PG (2005) A funneled energy landscape for cytochrome *c* directly predicts the sequential folding route inferred from hydrogen exchange experiments. Proc Natl Acad Sci USA 102: 12401–12406.
53. Milne JS, Xu Y, Mayne LC, Englander SW (1999) Experimental study of the protein folding landscape: unfolding reactions in cytochrome c. J Mol Biol 290: 811–822.
54. Hilser VJ. Modeling the native state ensemble. In: Murphy KP, Ed. (2001) Totowa, NJ: Humana Press, pp 93–116.
55. Hamburger JB, Hilser VJ (2004) Characterization of local fluctuations using hydrogen exchange. Biophys J 86:500A–501A.
56. Kubelka J, Hofrichter J, Eaton WA (2004) The protein folding "speed limit". Curr Opin Struct Biol 14:76–88.
57. Kubelka J, Buscaglia M, Hofrichter J, Eaton WA (2005) Ultrafast kinetic studies and the protein folding "Speed limit". NATO Sci Ser I: Life Behav Sci 364:1–10.
58. Gilson MK, Radford SE (2011) Protein folding and binding: from biology to physics and back again. Curr Opin Struct Biol 21:1–3.
59. Hoang L, Maity H, Krishna MM, Lin Y, Englander SW (2003) Folding units govern the cytochrome *c* alkaline transition. J Mol Biol 331:37–43.
60. Skinner JJ, Wood S, Shorter J, Englander SW, Black BE (2008) The Mad2 partial unfolding model: regulating mitosis through Mad2 conformational switching. J Cell Biol 183:761–768.
61. Whitten ST, Garcia-Moreno EB, Hilser VJ (2005) Local conformational fluctuations can modulate the coupling between proton binding and global structural transitions in proteins. Proc Natl Acad Sci USA 102: 4282–4287.
62. Hilser VJ, Garcia-Moreno B, Oas TG, Kapp G, Whitten ST (2006) A statistical thermodynamic model of the protein ensemble. Chem Rev 106:1545–1558.
63. Lindorff-Larsen K, Piana S, Dror RO, Shaw DE (2011) How fast-folding proteins fold. Science 334:517–520.